

MINIMUM ENERGY MAGNETIC FIELDS WITH TOROIDAL TOPOLOGY

A. Y. K. CHUI * and H. K. MOFFATT *
*Institute for Theoretical Physics
University of California
Santa-Barbara, California 93106-4030, U.S.A.*

ABSTRACT. Consider a flux tube initially constructed in an incompressible perfectly conducting fluid around an arbitrary knot K in a standard way such that the total helicity is prescribed; the minimum energy of the flux tube is then determined (in principle) solely by the topology of K . In this paper we restrict attention to axisymmetric configurations, so that K is a circle. The functional relationship between minimum energy (in axisymmetric relaxed states) and helicity is determined via a variational principle approach. The result is confirmed by considering the scaling properties of the Grad-Shafranov equation. We discuss briefly how this result is modified when non-axisymmetric equilibrium states are allowed.

1. Introduction

It has been shown (Moffatt 1990) that, if a tube of volume V and carrying magnetic flux Φ is constructed around an arbitrary knot K , in a standard way such that the helicity of the field is given by $\mathcal{H} = h\Phi^2$, then the minimum magnetic energy of the field under the group of volume-preserving distortions (realizable by incompressible flow) is given by

$$\mathcal{M}_{min} = m(h)\Phi^2V^{-1/3} \tag{1.1}$$

where $m(h)$ is a function determined (in principle) solely by the topology of K . If K is the 'unknot', then h is the twist (or 'rotational transform') of the magnetic field \mathbf{B} in the toroidal tube surrounding K . If we restrict attention to axisymmetric configurations, so that K is a circle, then we may seek to determine the function $m_a(h)$ corresponding to the minimum magnetic energy of axisymmetric field configurations with toroidal topology. These

* Permanent address: DAMTP, University of Cambridge, Silver Street, Cambridge CB3 9EW, England

axisymmetric configurations may be unstable to non-axisymmetric perturbations leading to lower energy equilibrium states. We may be confident however that $m_a(h)$ provides an upper bound for $m(h)$:

$$m(h) \leq m_a(h). \quad (1.2)$$

Determination of $m_a(h)$, which is the objective of the present paper, is an essential preliminary to the determination of $m(h)$; this in turn is an essential preliminary to determination of $m(h)$ for any knot K of nontrivial topology. We see this therefore as a first step in a program of increasing complexity.

There are however independent reasons for the study of axisymmetric configurations. Magnetic containment devices like the TOKAMAK are axisymmetric, and, in ideal circumstances, the magnetic field and the contained plasma adopt an axisymmetric magnetostatic configuration of minimum magnetic energy. Determination of such states is a classical problem of plasma physics (see, for example, Thompson 1962). These states are of course constrained by the particular geometry of the containment device and of the surrounding coils. Here we allow the toroidal flux tube to expand or contract in radius without any such constraint, the equilibrium state being determined solely by Φ, V and h ; this procedure gives some useful insight concerning configurations that may be regarded as 'natural' and therefore most easily containable.

The minimum energy states are magnetostatic equilibria satisfying the equations

$$\mathbf{j} \wedge \mathbf{B} = \nabla p, \quad \mu_0 \mathbf{j} = \nabla \wedge \mathbf{B} \quad \text{and} \quad \nabla \cdot \mathbf{B} = 0, \quad (1.3)$$

where \mathbf{j} is the current density and p is the pressure field. To each solution of these equations, there corresponds via the analogy $\mathbf{B} \leftrightarrow \mathbf{u}$, $\mu_0 \mathbf{j} \leftrightarrow \boldsymbol{\omega}$ and $p_0 - p \leftrightarrow \mu_0 h$, a solution of the steady Euler equations for incompressible flow:

$$\mathbf{u} \wedge \boldsymbol{\omega} = \nabla h, \quad \boldsymbol{\omega} = \nabla \wedge \mathbf{u} \quad \text{and} \quad \nabla \cdot \mathbf{u} = 0. \quad (1.4)$$

The states that we shall describe correspond to toroidal vortex configurations which are stationary relative to the surrounding fluid, in fact $\mathbf{u} \equiv \mathbf{0}$ outside the torus to which the vorticity is confined. The total flux of vorticity around the tube (including a surface contribution) is zero. They are thus a degenerate form of 'vortex tube with swirl'. There is no guarantee that these flows are stable, even to axisymmetric disturbances. They are nevertheless of peculiar interest as examples of steady axisymmetric Euler flow of finite energy in unbounded fluid.

In section 2, we recapitulate the construction of a standard twisted flux tube, as described by Moffatt (1990), and we give an explicit calculation of the associated helicity. In section 3, we reformulate the minimum energy

variational principle, incorporating the helicity and incompressibility constraints. In sections 4 and 5, we obtain asymptotic expressions for $m_a(h)$ for $h \gg 1$ and $h \ll 1$ respectively, and in section 6, we present the results of numerical calculation based on the variational principle, which confirm the asymptotic results, and we determine $m_a(h)$ in the transitional regime when $h = O(1)$. In section 7, the asymptotic results are interpreted in terms of appropriate scalings of the Grad-Shafranov equation; and in section 8, the results are summarised, and we discuss qualitatively the nature of the non-axisymmetric instabilities to which the equilibrium states may be subject.

2. Construction of Flux Tube of Prescribed Helicity

Let \mathcal{T} be the torus defined by

$$\mathcal{T} = \{(r, \theta, z) : (r - R)^2 + z^2 \leq (\varepsilon R)^2\} \quad (2.1)$$

where $\varepsilon \leq 1$. The cross-section \mathcal{A} of this torus is circular with area $A = \pi \varepsilon^2 R^2$, and its volume is

$$V = \int_{\mathcal{A}} 2\pi r \, dr \, dz = 2\pi AR = 2\pi^2 \varepsilon^2 R^3. \quad (2.2)$$

We now define a toroidal field $\mathbf{B}_T = (0, B, 0)$ given by

$$B = \begin{cases} 2\pi r \Phi / V & \text{inside } \mathcal{T}; \\ 0 & \text{otherwise.} \end{cases} \quad (2.3)$$

The toroidal flux of this field using (2.2) is

$$\int_{\mathcal{A}} 2\pi r \Phi / V \, dr \, dz = \Phi. \quad (2.4)$$

Note that $B/r = 2\pi \Phi / V$ is constant; under any volume-preserving axisymmetric frozen-field distortion, B/r is constant following a given field line; hence the field (2.3) is invariant in form within the tube \mathcal{T} if the tube is radially expanded or contracted. It is moreover the unique field (of flux Φ) with this property.

We now wish to construct an associated poloidal field \mathbf{B}_P by simple surgery as follows: imagine that we cut the flux tube at the section $\theta = 0$, twist the tube as if to make a twisted rope, the twist being uniformly distributed with respect to the angle θ , and then reconnect the flux tube (figure 1). Let us calculate the field \mathbf{B}_P generated by this operation.

The velocity field that provides the required twisting effect is

$$\mathbf{v}(r, \theta, z) = \frac{\theta}{2\pi} \left(-\frac{1}{r} \frac{\partial \psi}{\partial z}, 0, \frac{1}{r} \frac{\partial \psi}{\partial r} \right) \stackrel{\text{def}}{=} \frac{\theta}{2\pi} \hat{\mathbf{v}}, \quad (0 < \theta \leq 2\pi); \quad (2.5)$$

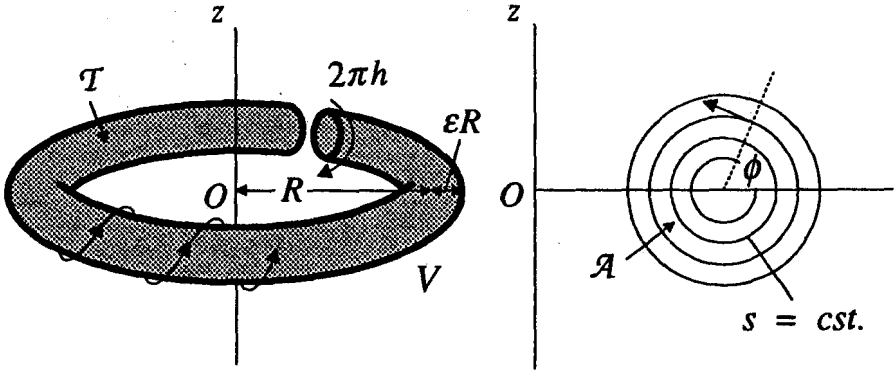


Fig. 1. The simple surgery consists of three steps: cutting the tube, twisting it uniformly and reconnecting it.

where $\psi = \psi(r, z)$ is the Stokes stream function of $\hat{\mathbf{v}}$. Note that \mathbf{v} satisfies the incompressibility condition $\nabla \cdot \mathbf{v} = 0$, and is discontinuous across the cut at $\theta = 0$. We choose

$$\psi(r, z) = \begin{cases} \frac{1}{2}\psi_0((r - R)^2 + z^2) & \text{inside } \mathcal{T}, \\ 0 & \text{otherwise;} \end{cases} \tag{2.6}$$

so that the streamlines in any plane $\theta = cst.$ are circles centred on $(r, z) = (R, 0)$. We will find it useful (see figure 1) to define the polar coordinates (s, ϕ) such that

$$r - R = s \cos \phi, \quad z = s \sin \phi; \tag{2.7}$$

then the velocity of the fluid particle on the circle of radius s at the plane $\theta = 2\pi$ is $v_\phi = \psi_0 s / r$, and the time to describe a complete circle is

$$T = \oint \frac{s d\phi}{v_\phi} = \frac{1}{\psi_0} \oint (s \cos \phi + R) d\phi = \frac{2\pi R}{\psi_0}, \tag{2.8}$$

independent of s .

Consider now the action of the velocity field (2.5) on the field (2.3). Let $\mathbf{B}(\mathbf{x}, t) = \mathbf{B}_T(\mathbf{x}, t) + \mathbf{B}_P(\mathbf{x}, t)$ be the magnetic field at time t . From the frozen-field equation,

$$\frac{\partial \mathbf{B}}{\partial t} = \nabla \wedge (\mathbf{v} \wedge \mathbf{B}) = (\Phi/V) \hat{\mathbf{v}}, \tag{2.9}$$

and this field is axisymmetric and poloidal: only poloidal field is generated by the surgery, and the toroidal field is left invariant. At time $t = hT = 2\pi h R / \psi_0$ (when the tube is twisted through h turns),

$$\mathbf{B}_P = \frac{2\pi h R \Phi}{\psi_0 V} \hat{\mathbf{v}} \stackrel{\text{def}}{=} \nabla \wedge \mathbf{A}_T, \quad (2.10)$$

where

$$\mathbf{A}_T = \begin{cases} \left(0, \frac{\pi R h \Phi}{r V} ((r - R)^2 + z^2), 0\right) & \text{inside } \mathcal{T}, \\ \mathbf{0} & \text{otherwise;} \end{cases} \quad (2.11)$$

and the total poloidal flux generated between the magnetic axis $s = 0$ and the tube boundary $s = \varepsilon R$ is then $\Phi_P = h\Phi$.

The helicity of the field can now be easily calculated. Note first that, with $\mathbf{B}_T = \nabla \wedge \mathbf{A}_P$,

$$\int \mathbf{B}_T \cdot \mathbf{A}_P dV = \int \mathbf{B}_P \cdot \mathbf{A}_T dV = 0 \quad (2.12)$$

and

$$\int \mathbf{B}_T \cdot \mathbf{A}_T dV = \int \mathbf{B}_P \cdot \mathbf{A}_P dV; \quad (2.13)$$

hence

$$\begin{aligned} \mathcal{H} &= \int \mathbf{A} \cdot \mathbf{B} dV = 2 \int_{\mathcal{T}} \mathbf{A}_T \cdot \mathbf{B}_T dV \\ &= \frac{2\pi h R \Phi^2}{V^2} \int_{\mathcal{T}} \left((r - R)^2 + z^2 \right) r dr dz \quad \text{using (2.3) and (2.11)} \\ &= \frac{2\pi h R \Phi^2}{(\pi \varepsilon^2 R^3)^2} \int_0^{2\pi} \int_0^{\varepsilon R} s^2 (s \cos \phi + R) s ds d\phi \quad \text{using (2.7)} \\ &= h\Phi^2 = \Phi\Phi_P. \end{aligned} \quad (2.14)$$

When $h = 1$, then every pair of \mathbf{B} -lines are linked with linking number +1, and the result $\mathcal{H} = \Phi^2$ may be obtained in this case from the formula [Moffatt 1990]

$$\mathcal{H} = 2 \int_0^\Phi \varphi d\varphi = \Phi^2. \quad (2.15)$$

Hence (2.14) merely confirms what may be physically obvious. Note that if $h = p/q$ is rational (where p and q are co-prime integers), then each \mathbf{B} -line (except the 'magnetic axis' $s = 0$) is a torus knot $K_{p,q}$. If h is irrational, then (with the same exception) each \mathbf{B} -line covers a torus $s = \text{cst}$. In the context of toroidal containment devices, h is known as the 'rotational transform' and the nested tori defined by \mathbf{B} -lines are called magnetic surfaces.

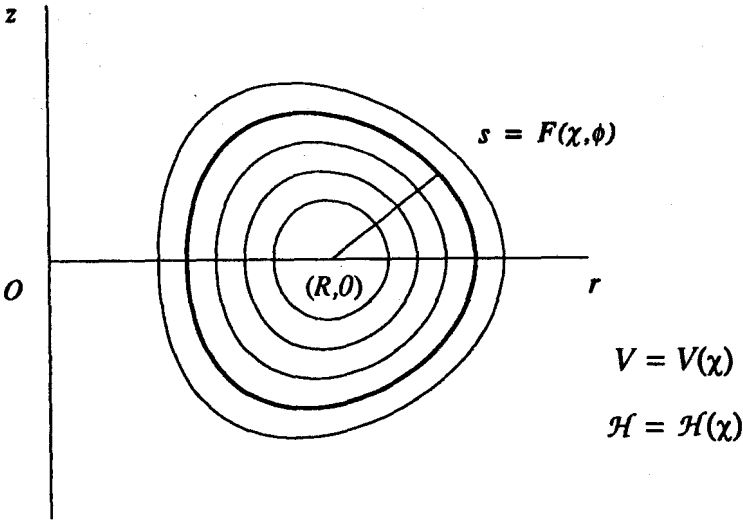


Fig. 2. The magnetic energy is minimised subject to two families of constraints which fix the volume $V(\chi)$ and the helicity $\mathcal{H}(\chi)$ inside each magnetic surface $\chi = cst.$

3. The Variational Principle

In this section, we shall develop the necessary tool for the problem. There are two approaches for obtaining relaxed states: we can follow the dynamical process directly using the MHD equations and including viscous (or equivalent) dissipation of energy; or we can make use of the fact that the relaxed state has minimum energy, which leads to a variational principle. In this paper we will adopt the second approach. It is known (Moffatt 1969) that the helicity is conserved inside each magnetic surface, and the incompressibility condition implies that the volume is also conserved inside each magnetic surface. Expressing \mathbf{B} in the standard way

$$\mathbf{B} = \mathbf{B}_T + \mathbf{B}_P = \left(0, B(r, z), 0\right) + \left(-\frac{1}{r} \frac{\partial \chi(r, z)}{\partial z}, 0, \frac{1}{r} \frac{\partial \chi(r, z)}{\partial r}\right) \quad (3.1)$$

where $\chi = cst.$ on the magnetic surfaces, we may formulate the variational principle as follows. Let $(R, 0)$ be the position of the elliptic point (at which $\chi = 0$) in the $(r-z)$ plane at equilibrium. Define the polar coordinates (s, ϕ) with the origin at $(R, 0)$ as in (2.7). Let

$$s = F(\chi, \phi) \quad (3.2)$$

be the contours of constant χ (figure 2). It is required to

Minimise

$$\mathcal{M} = \frac{1}{2} \int \mathbf{B}^2 dV = \frac{1}{2} \int \left[B^2 + \frac{1}{r^2} \left(\left(\frac{\partial \chi}{\partial r} \right)^2 + \left(\frac{\partial \chi}{\partial z} \right)^2 \right) \right] dV \quad (3.3)$$

subject to

$$\int_{s \leq F(\chi, \phi)} dV = V(\chi) \quad (3.4)$$

and

$$\int_{s \leq F(\chi, \phi)} \mathbf{B} \cdot \mathbf{A} dV = \int_{s \leq F(\chi, \phi)} 2 \mathbf{B}_T \cdot \mathbf{A}_T dV = \int_{s \leq F(\chi, \phi)} \frac{2B\chi}{r} dV = \mathcal{H}(\chi) \quad (3.5)$$

where $V(\chi)$ and $\mathcal{H}(\chi)$ are prescribed. Here $B = B(s, \phi)$, $F = F(\chi, \phi)$ and $R = cst.$ are to be determined. Note that (3.4) and (3.5) are two functional constraints which represent the infinite number of constraints on magnetic surfaces $\chi = cst.$, $0 \leq \chi \leq \chi_{max}$. This formulation of the problem is equivalent to that of Kruskal & Kulsrud (1958) who however expressed the constraints entirely in terms of flux and mass conservation.

Let us examine (3.3) in more detail. First note that

$$\begin{aligned} \frac{\partial \chi}{\partial r} &= \frac{\partial \chi}{\partial s} \frac{\partial s}{\partial r} + \frac{\partial \chi}{\partial \phi} \frac{\partial \phi}{\partial r} = \frac{\cos \phi}{F_\chi} + \frac{F_\phi \sin \phi}{F_\chi s}, \\ \frac{\partial \chi}{\partial z} &= \frac{\partial \chi}{\partial s} \frac{\partial s}{\partial z} + \frac{\partial \chi}{\partial \phi} \frac{\partial \phi}{\partial z} = \frac{\sin \phi}{F_\chi} - \frac{F_\phi \cos \phi}{F_\chi s}; \end{aligned} \quad (3.6)$$

hence, with (2.7) and (3.2), we simplify (3.3) to

$$\mathcal{M} = \pi \int_0^{2\pi} \int_0^{\chi_{max}} \left(G^2 (R + F \cos \phi) F F_\chi + \frac{F^2 + F_\phi^2}{(R + F \cos \phi) F F_\chi} \right) d\chi d\phi \quad (3.7)$$

where

$$G(\chi, \phi) \equiv B(F(\chi, \phi), \phi). \quad (3.8)$$

Now we manipulate (3.4) in the same way to obtain

$$2\pi \int_0^{2\pi} \int_0^\chi (R + F(\chi', \phi) \cos \phi) F(\chi', \phi) F_{\chi'}(\chi', \phi) d\chi' d\phi = V(\chi) \quad (3.9)$$

and differentiate to obtain

$$\frac{1}{2\pi}V'(\chi) = \int_0^{2\pi} (R + F \cos \phi) F F_\chi d\phi. \quad (3.10)$$

Similarly, (3.5) leads to

$$\int_0^{2\pi} G F F_\chi d\phi = \frac{1}{4\pi\chi} \mathcal{H}'(\chi). \quad (3.11)$$

The constraints (3.9) and (3.11) mean simply that the volume and helicity between any two neighbouring magnetic surfaces are prescribed and fixed.

The function G can be determined by the usual Lagrange multiplier technique: if $\lambda(\chi)$ is the Lagrange multiplier for the constraint (3.11), we immediately find that

$$G = \frac{\lambda(\chi)}{2(R + F \cos \phi)} \quad (3.12)$$

where, from (3.11), $\lambda(\chi)$ satisfies

$$\lambda \int_0^{2\pi} \frac{F F_\chi d\phi}{2(R + F \cos \phi)} = \frac{\mathcal{H}'(\chi)}{4\pi\chi}. \quad (3.13)$$

Note that the first term in (3.3) becomes

$$\begin{aligned} \mathcal{M}_1 &= \pi \int_0^{\chi_{max}} \frac{\lambda}{2} \int_0^{2\pi} \frac{\lambda F F_\chi}{2(R + F \cos \phi)} d\phi d\chi = \pi \int_0^{\chi_{max}} \frac{\lambda}{2} \frac{\mathcal{H}'(\chi)}{4\pi\chi} d\chi \\ &= \pi \int_0^{\chi_{max}} \left(\frac{\mathcal{H}'(\chi)}{4\pi\chi} \right)^2 \left(\int_0^{2\pi} \frac{F F_\chi d\phi}{(R + F \cos \phi)} \right)^{-1} d\chi. \end{aligned} \quad (3.14)$$

The analysis so far is applicable to all axisymmetric fields with magnetic surfaces in the form of nested tori. For the particular case of the flux tube defined in section 2 we may calculate $V(\chi)$, $\mathcal{H}(\chi)$ and χ_{max} explicitly. From (2.11), we see that then (using $\mathbf{A}_T = (0, \chi/r, 0)$),

$$s = \left(\frac{\chi V}{h\pi R\Phi} \right)^{\frac{1}{2}} \stackrel{\text{def}}{=} S(\chi). \quad (3.15)$$

Note that s attains its maximum εR when $\chi = \chi_{max}$, so that

$$\chi_{max} = h\pi R (\varepsilon R)^2 \frac{\Phi}{V} = \frac{h\Phi}{2\pi}. \quad (3.16)$$

Using (3.15), we now obtain

$$\begin{aligned} V(\chi) &= 2\pi \iint_{s \leq S(\chi)} r dr dz = 2\pi \iint_{s \leq S(\chi)} (R + s \cos \phi) s ds d\phi \\ &= 4\pi^2 R \left[\frac{s^2}{2} \right]_0^{S(\chi)} = \frac{2\pi\chi V}{h\Phi} \end{aligned} \quad (3.17)$$

and similarly

$$\mathcal{H}(\chi) = \frac{4\pi^2}{h} \chi^2. \quad (3.18)$$

Note that $V(\chi_{max}) = V$ and the total helicity $\mathcal{H}(\chi_{max}) = h\Phi^2$ as expected. The variational problem now becomes:

Find the function $F(\chi, \phi)$ and the constant R that minimise

$$\mathcal{M} = \pi \int_0^{\chi_{max}} \left[\frac{4\pi^2}{h^2} \left(\int_0^{2\pi} \frac{FF_\chi d\phi}{R + F \cos \phi} \right)^{-1} + \int_0^{2\pi} \frac{(F^2 + F_\phi^2) d\phi}{(R + F \cos \phi) FF_\chi} \right] d\chi \quad (3.19)$$

subject to the constraint

$$\int_0^{2\pi} (R + F \cos \phi) FF_\chi d\phi = \frac{V}{h\Phi}. \quad (3.20)$$

This variational problem cannot be solved analytically. However, by restricting $F(\chi, \phi)$ to be within a certain class of functions, it is possible to obtain an upper bound for the true minimum. In the following sections, we will study, in turn, the cases of (i) large h , (ii) small h and (iii) $h = O(1)$.

4. The Case of Large h

In this section the minimum energy of the flux tube in the large h limit will be examined. In the order of complexity, we use three different methods to provide successively better estimates of the true minimum from above. A lower bound for the true minimum energy will also be estimated using the Poincaré inequality.

4.1. THE SCALING ARGUMENT

Consider the flux tube confined in the torus \mathcal{T} as described in (2.1), carrying a magnetic field $\mathbf{B} = \mathbf{B}_T + \mathbf{B}_P$. Recall that R is the mean radius of the flux tube and A is the area of the cross-section \mathcal{A} . Let $\Phi = \int_{\mathcal{A}} |\mathbf{B}_T(r, z)| dr dz$ be the toroidal flux of \mathbf{B} around Oz . Under any volume-preserving axisymmetric frozen-field distortion, both V (the volume of the tube) and Φ are invariant. If, for example, the tube is stretched so that R increases, then A decreases so that $V = 2\pi RA = cst$.

Under such a distortion, $|\mathbf{B}_T|$ increases in proportion to R ; if the distortion is such that A contracts in self-similar manner, then $|\mathbf{B}_P|$ decreases in proportion to $A^{\frac{1}{2}}$; also if the poloidal field is generated by the cut-and-twist surgery as described in section 2, then $|\mathbf{B}_P|$ is proportional to h . On dimensional ground we therefore have

$$|\mathbf{B}_T| \sim \Phi V^{-1} R, \quad |\mathbf{B}_P| \sim h\Phi(VR)^{-1/2}; \quad (4.1)$$

and the magnetic energy may be written in the form

$$\mathcal{M} = k_T \frac{\Phi^2}{V} R^2 + k_P \Phi^2 \frac{h^2}{R} \quad (4.2)$$

where k_T and k_P are dimensionless constants. Hence \mathcal{M} is minimal when

$$R = (k_P/2k_T)^{\frac{1}{3}} V^{\frac{1}{3}} h^{\frac{2}{3}} \quad (4.3)$$

and then

$$\mathcal{M}_{min} \sim h^{\frac{4}{3}} \Phi^2 / V^{\frac{1}{3}} \quad (4.4)$$

for some constant k . Since h , Φ and V are invariant under all frozen field distortions of the flux-tube, this provides an important estimate (to within a constant of order unity) of the minimum magnetic energy that may be attained.

4.2. EVALUATING THE ENERGY INTEGRALS

With the magnetic field explicitly defined in section 2, we now calculate the energy

$$\mathcal{M} = \mathcal{M}_T + \mathcal{M}_P = \frac{1}{2} \int \mathbf{B}_T^2 dV + \frac{1}{2} \int \mathbf{B}_P^2 dV \quad (4.5)$$

of the twisted flux tube constructed as above. Firstly,

$$\begin{aligned} \mathcal{M}_T &= \frac{1}{2} \int_{\mathcal{A}} (2\pi r)^2 \frac{\Phi^2}{V^2} 2\pi r dr dz \\ &= 4\pi^3 \frac{\Phi^2}{V^2} \int_0^{2\pi} \int_0^{\epsilon R} (R + s \cos \phi)^3 s ds d\phi \quad \text{using (2.7)} \\ &= \frac{2\pi^2 R^2 \Phi^2}{V} \left(1 + \frac{3}{4} \epsilon^2 \right). \end{aligned} \quad (4.6)$$

The first term dominates when $\epsilon \ll 1$ (so that the tube is thin and long), and corresponds to the energy of a uniform flux tube of length $2\pi R$; the second term is the correction associated with the fact that the axis of the tube is curved, with radius of curvature R .

Secondly, since from (2.10) and (2.11),

$$\mathbf{B}_P^2 = \left(2\pi R h \frac{\Phi s}{V r} \right)^2, \quad (4.7)$$

the poloidal energy is given by

$$\begin{aligned} \mathcal{M}_P &= \frac{\pi \Phi^2}{V^2} \int_0^{2\pi} \int_0^{\epsilon R} \frac{4\pi^2 R^2 s^2 h^2}{R + s \cos \phi} s ds d\phi \\ &= \frac{2^{\frac{4}{3}} \pi^{\frac{2}{3}} \Phi^2 h^2}{3V^{\frac{1}{3}}} \epsilon^{-\frac{10}{3}} \left(2 - (1 - \epsilon^2)^{\frac{1}{2}} (2 + \epsilon^2) \right). \end{aligned} \quad (4.8)$$

Note here the limiting form for small ϵ

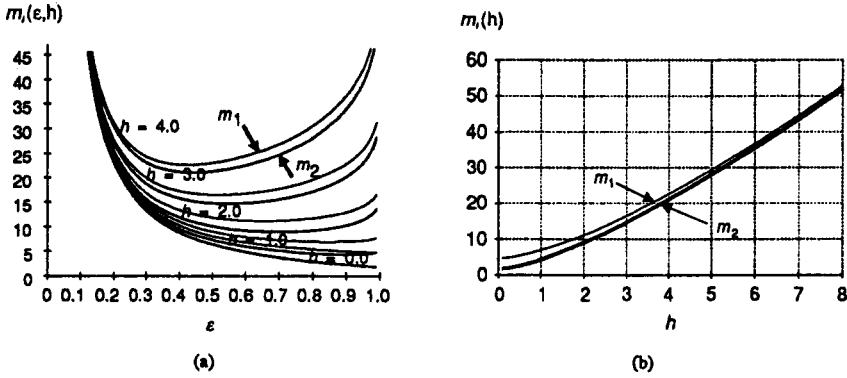


Fig. 3. (a) magnetic energy $m_1(\epsilon, h)$ and $m_2(\epsilon, h)$ are plotted against ϵ for various values of h ; (b) the minimum energy $\min_{\epsilon} m_1(\epsilon, h)$ and $\min_{\epsilon} m_2(\epsilon, h)$ are plotted against h .

$$\mathcal{M}_P \approx \frac{2^{\frac{4}{3}} \pi^{\frac{2}{3}} \Phi^2 h^2}{3V^{\frac{1}{3}}} \epsilon^{-\frac{10}{3}} \times \frac{3}{8} \epsilon^4 = \frac{h^2 \Phi^2}{2R} \quad \text{as } \epsilon \rightarrow 0 \quad (4.9)$$

(cf. 4.2). We now have

$$\mathcal{M} = \frac{\Phi^2}{V^{\frac{1}{3}}} m_1(\epsilon, h) \quad (4.10)$$

where

$$m_1(\epsilon, h) = \frac{2^{\frac{1}{3}} \pi^{\frac{2}{3}}}{\epsilon^{\frac{4}{3}}} \left(1 + \frac{3}{4} \epsilon^2 + \frac{2h^2}{3\epsilon^2} \left(2 - (1 - \epsilon^2)^{\frac{1}{2}} (2 + \epsilon^2) \right) \right). \quad (4.11)$$

This function is sketched in figure 3 for $0 < \epsilon \leq 1$ and various values of h . Note the presence of a minimum value for all $h \neq 0$ (since $\partial m_1 / \partial \epsilon < 0$ as $\epsilon \rightarrow 0$, but > 0 as $\epsilon \rightarrow 1$).

For $h \gg 1$, m_1 attains its minimum when $\epsilon \ll 1$, so \mathcal{M}_{min} may be expanded in an asymptotic series (for small ϵ)

$$\mathcal{M} \approx \frac{2^{\frac{1}{3}} \pi^{\frac{2}{3}} \Phi^2}{V^{\frac{1}{3}}} \epsilon^{-\frac{4}{3}} \left(1 + \left(\frac{3}{4} + \frac{1}{2} h^2 \right) \epsilon^2 + \dots \right) \quad (4.12)$$

which has a minimum when

$$\epsilon^2 = \frac{8}{3 + 2h^2} \approx 4/h^2, \quad (4.13)$$

or equivalently when

$$R = R_{min} \approx \frac{1}{2} \left(\frac{Vh^2}{\pi} \right)^{\frac{1}{3}} \quad (4.14)$$

(cf. 4.3), and then

$$\mathcal{M} = \mathcal{M}_{min} \approx \frac{3\pi^{\frac{2}{3}} h^{\frac{4}{3}} \Phi^2}{2 V^{\frac{1}{3}}} \approx 3.22 h^{\frac{4}{3}} \frac{\Phi^2}{V^{\frac{1}{3}}}, \quad (4.15)$$

in confirmation of the previous estimates (4.3) and (4.4).

4.3. THE ENERGY PRINCIPLE

In the above calculation, we have assumed that the tube cross-section is circular, and the field structure is invariant. We ignored the fact that the toroidal field may be re-distributed during the relaxation, even if each magnetic surface is constrained to have circular cross-section. We now calculate the effect of this redistribution.

Consider the variational principle (3.19)–(3.20) in the case of circular cross-sections. For large h we assume that F is independent of ϕ , so each contour with constant χ is circular; then (3.19) yields

$$FF_\chi = \frac{V}{2\pi h \Phi R} \quad (4.16)$$

and hence

$$F^2 = \frac{V\chi}{\pi h \Phi R}. \quad (4.17)$$

Now we have to minimise

$$\mathcal{M} = 4\pi^2 \int_0^{\chi_{max}} \left(\frac{\pi R \Phi}{hV} (R^2 - F^2) + \chi \right) \frac{d\chi}{\sqrt{R^2 - F^2}} \quad (4.18)$$

where $\chi_{max} = h\Phi/2\pi$ and F is given by (4.17). The integral can be evaluated to give

$$\mathcal{M} = \frac{\Phi^2}{V^{\frac{1}{3}}} m_2(\varepsilon, h) \quad (4.19)$$

where

$$m_2(\varepsilon, h) = 2^{\frac{4}{3}} \pi^{\frac{2}{3}} \varepsilon^{-\frac{10}{3}} \left(\frac{1-h^2}{3} (1 - (1-\varepsilon^2)^{\frac{3}{2}}) + h^2 (1 - (1-\varepsilon^2)^{\frac{1}{2}}) \right) \quad (4.20)$$

is to be minimised. This function (figure 3) provides an estimate of minimum energy less than that given in (4.11): in that calculation, the structure of the toroidal field was prescribed and fixed, so that the class of equilibrium states to which the tube could relax was narrowed. We also note that now the relaxed toroidal field is $(0, B_E(r, z), 0)$, where

$$B_E(r, z) = 2\pi R \frac{\Phi}{V} \frac{\sqrt{2rR - r^2 - z^2}}{r} \quad (4.21)$$

using (3.8), (3.12) and (3.13). However, the asymptotic form of $m_2(\varepsilon, h)$ for small ε is

$$m_2(\varepsilon, h) = 2^{\frac{4}{3}} \pi^{\frac{2}{3}} \varepsilon^{-\frac{10}{3}} \left(\frac{1}{2} \varepsilon^2 + \frac{2h^2 - 1}{8} \varepsilon^4 + \dots \right) \quad (4.22)$$

which has a minimum when

$$\varepsilon^2 \approx 4/h^2, \quad (4.23)$$

and then $\mathcal{M}_{min} = kh^{\frac{4}{3}}$ (with same constant k as before). These results are the same as given in (4.13)–(4.15): when $h \gg 1$, the area of cross-section is $O(R^{-1})$, so the details of the toroidal field distribution become unimportant.

4.4. THE LOWER BOUND

There is also a lower bound on the magnetic energy when $h \neq 0$ [Arnol'd 1974, Moffatt 1985, Freedman 1988]. This results from the Schwarz inequality

$$\int \mathbf{B}^2 dV \cdot \int \mathbf{A}^2 dV \geq \left(\int \mathbf{A} \cdot \mathbf{B} dV \right)^2 \quad (4.24)$$

and the Poincaré inequality

$$\frac{\int \mathbf{B}^2 dV}{\int \mathbf{A}^2 dV} \geq q_0^2 \quad (4.25)$$

where q_0 is a constant (with dimensions $(\text{length})^{-1}$) depending on the geometry of the fluid domain. Hence

$$\int \mathbf{B}^2 dV \geq q_0 \left| \int \mathbf{A} \cdot \mathbf{B} dV \right|. \quad (4.26)$$

Writing

$$\mathcal{M} = \frac{1}{2} \int \mathbf{B}^2 dV = m_a(h) \frac{\Phi^2}{V^{\frac{1}{3}}} \quad (4.27)$$

and

$$\mathcal{H} = \int \mathbf{A} \cdot \mathbf{B} dV = h \Phi^2, \quad (4.28)$$

we then have

$$m_a(h) \geq \frac{1}{2} q_0 V^{\frac{1}{3}} |h|. \quad (4.29)$$

For example ¹, the fluid domain may be chosen to be a sphere of radius

$$R' = R(1 + \varepsilon) = \left(\frac{V}{2\pi^2\varepsilon^2} \right)^{\frac{1}{3}} (1 + \varepsilon), \quad (4.30)$$

which just contains the flux tube. Then $q_0 = \pi/R'$, so that (4.29) becomes

$$m_a(h) \geq 2^{-\frac{2}{3}} \pi^{\frac{5}{3}} |h| \frac{\varepsilon^{\frac{2}{3}}(h)}{1 + \varepsilon(h)}. \quad (4.31)$$

In the limit $h \rightarrow \infty$, $\varepsilon \rightarrow 2/h$ so that

$$m_a(h) \geq \pi^{\frac{5}{3}} |h^{\frac{1}{3}}| \quad (4.32)$$

approximately. Combining this with the previous result, we have

$$\pi^{\frac{5}{3}} h^{\frac{1}{3}} \leq m_a(h) \leq \frac{3\pi^{\frac{2}{3}}}{2} h^{\frac{4}{3}} \quad (4.33)$$

in the limit $h \rightarrow \infty$.

5. THE CASE OF SMALL h

In the case of small h the poloidal field is weak; the toroidal field then tends to contract and give up energy, and hence to squeeze the flux tube onto the axis of symmetry. The cross-section is then long and thin, and the flux tube may be approximated by a hollow cylinder

$$C = \{(r, \theta, z) : R - \varepsilon R < r < R + \varepsilon R, |z| < L\} \quad (5.1)$$

(see figure 4a), of volume $V = 8\pi\varepsilon R^2 L$, $\varepsilon \leq 1$, with $R \ll L$. We shall assume that $\varepsilon = O(1)$ as $h \rightarrow 0$.

5.1. THE SCALING ARGUMENT

Let

$$\mathbf{B} = \left(B_r, 2\pi r \frac{\Phi}{V}, B_z \right) \quad (5.2)$$

so that the total toroidal flux is invariant. The toroidal energy has the same scaling property

$$\mathcal{M}_T = \frac{1}{2} \int |\mathbf{B}_T|^2 dV \sim \frac{R^2 \Phi^2}{V} \quad (5.3)$$

¹ This provides a rather poor lower bound when $h \gg 1$; a better lower bound could be obtained by, for example, taking the fluid domain to be the spherical annulus $R(1 - \varepsilon) < r < R(1 + \varepsilon)$. The important point, however, is that there is *always* a positive lower bound for the energy when $h \neq 0$

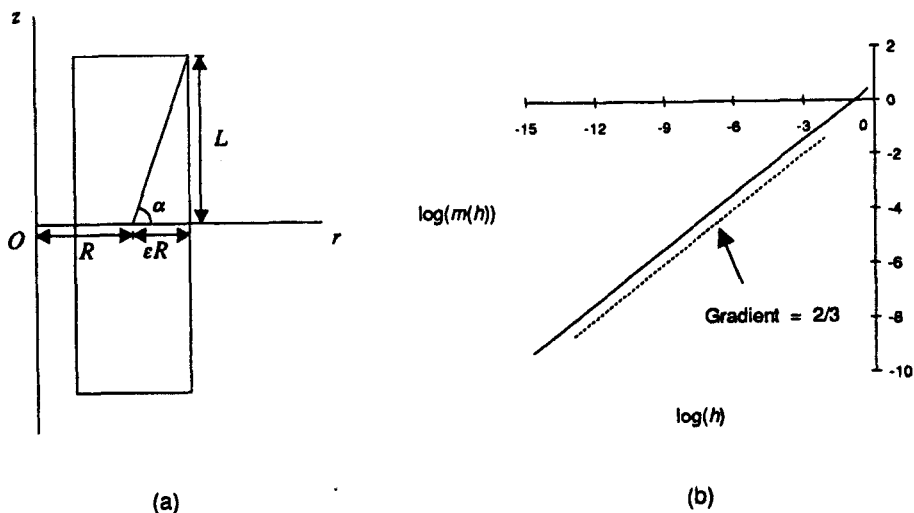


Fig. 4. (a) when h is small, the flux tube is approximated by a hollow cylinder, hence it has rectangular cross-section; (b) $\log m_a(h)$ is plotted against $\log h$, showing that $m_a(h) = O(h^{2/3})$ in the limit $h \rightarrow 0$.

as before; the poloidal energy, however, scales differently. First note that the poloidal flux Φ_P about the magnetic axis can be estimated in two ways: it is the total flux across the ring $\{(r, \theta, z) : R < r < (1 + \epsilon)R, z = 0\}$ so that

$$|\Phi_P| \approx 2\pi R^2 |B_z| \quad (5.4)$$

or it is the total flux across the surface $\{(r, \theta, z) : r = R, 0 < z < L\}$ so that

$$|\Phi_P| \approx 2\pi RL |B_r| \quad (5.5)$$

where $|B_z|$ and $|B_r|$ are the average values. It follows that

$$\left| \frac{B_r}{B_z} \right| \sim \frac{R}{L}, \quad (5.6)$$

i.e. $|B_r| \ll |B_z|$. Using $\Phi_P = h\Phi$, the poloidal magnetic energy is then

$$\mathcal{M}_P = \frac{1}{2} \int (B_r^2 + B_z^2) dV \sim k_P \frac{h^2 \Phi^2 V}{R^4}. \quad (5.7)$$

Combining (5.3) and (5.7), the total magnetic energy is then

$$\mathcal{M} = k_T \frac{R^2 \Phi^2}{V} + k_P \frac{h^2 \Phi^2 V}{R^4} \quad (5.8)$$

where k_T and k_P are constants. This has a minimum when

$$R = \left(\frac{2k_P}{k_T} \right)^{\frac{1}{6}} h^{\frac{1}{3}} V^{\frac{1}{3}} \quad (5.9)$$

and then

$$\mathcal{M}_{min} \sim h^{\frac{2}{3}} \Phi^2 / V^{\frac{1}{3}}. \quad (5.10)$$

Note the different scalings of the minimum energy

$$\mathcal{M}_{min} = \begin{cases} O\left(h^{\frac{2}{3}}\right), & \text{when } h \text{ is small;} \\ O\left(h^{\frac{4}{3}}\right), & \text{when } h \text{ is large.} \end{cases} \quad (5.11)$$

5.2. THE VARIATIONAL PRINCIPLE

We assume that the magnetic surfaces are similar in shape, and that each takes the form of a hollow cylinder as described above. Hence we define

$$F(\chi, \phi) = \begin{cases} +\frac{f(\chi)}{\cos \phi}, & \phi \leq \alpha; \\ \frac{f(\chi)}{\sin \phi} \tan \alpha, & \alpha \leq \phi \leq \pi - \alpha; \\ -\frac{f(\chi)}{\cos \phi}, & \pi - \alpha < \phi \leq \pi; \end{cases} \quad (5.12)$$

where $\tan \alpha = L(\epsilon R)^{-1}$ (figure 4a), and $f(\chi)$ is an arbitrary function of χ . The integral in the constraint (3.20) can now be evaluated, and is simplified to

$$f f_\chi = \frac{V}{8R h \Phi \tan \alpha} = \frac{\pi \epsilon^2 R^2}{h \Phi} \quad (5.13)$$

so that

$$f^2 = \frac{2\pi \epsilon^2 R^2 \chi}{h \Phi}. \quad (5.14)$$

Hence the arbitrary function $f(\chi)$ is completely determined by the (volume) constraint. Using this result, and the normalizations

$$\chi \rightarrow \frac{h \Phi}{2\pi} \chi, \quad R \rightarrow V^{\frac{1}{3}} R; \quad (5.15)$$

we simplify (3.19) and obtain

$$\mathcal{M} = \frac{\Phi^2}{V^{\frac{1}{3}}} \int_0^1 \left(4\pi^2 R^2 J_1^{-1} + h^2 J_2 \right) d\chi \quad (5.16)$$

where

$$J_1 = \frac{1}{1 - \varepsilon^2 \chi} + \frac{1}{\varepsilon \chi^{\frac{1}{2}}} \tanh^{-1}(\varepsilon \chi^{\frac{1}{2}}),$$

$$J_2 = \frac{\chi}{4\pi^2 \varepsilon^2 (1 - \varepsilon^2 \chi) R^4} + 16\varepsilon \chi^{\frac{1}{2}} R^2 \tanh^{-1}(\varepsilon \chi^{\frac{1}{2}}); \quad (5.17)$$

and (5.22) is minimised subject to

$$R > 0, \quad 0 < \varepsilon < 1. \quad (5.18)$$

This has been done numerically, and $\log m_a(h)$ is plotted against $\log h$ in figure 4b. The slope is 2/3, confirming the estimate (5.11); we also found that $\varepsilon \not\rightarrow 1$ as $h \rightarrow 0$ (see below). However, if it were assumed that the contours are elliptic at the equilibrium state, then the closest distance between the outermost contour and the central axis should tend to zero.

In fact we can now prove the assertion that $\mathcal{M}_{\min} = O(h^{2/3})$ for small h . Defining

$$A(\varepsilon) = \int_0^1 4\pi^2 \left(\frac{1}{1 - \varepsilon^2 \chi} + \frac{1}{\varepsilon \chi^{\frac{1}{2}}} \tanh^{-1}(\varepsilon \chi^{\frac{1}{2}}) \right)^{-1} d\chi,$$

$$B(\varepsilon) = \int_0^1 \frac{\chi d\chi}{4\pi^2 \varepsilon^2 (1 - \varepsilon^2 \chi)},$$

$$C(\varepsilon) = \int_0^1 16\varepsilon \chi^{\frac{1}{2}} \tanh^{-1}(\varepsilon \chi^{\frac{1}{2}}) d\chi, \quad (5.19)$$

then (5.22) becomes

$$m_a(R, \varepsilon, h) = R^2(A(\varepsilon) + h^2 C(\varepsilon)) + \frac{h^2}{R^4} B(\varepsilon) \quad (5.20)$$

where $\mathcal{M} = \Phi^2 V^{-1/3} m_a$ as before. For any fixed ε , assuming that $A(\varepsilon)$, $B(\varepsilon)$ and $C(\varepsilon)$ are $O(1)$, then $m_a(R, \varepsilon, h)$ is minimal when $R = R^*$, where

$$R^{*2} = h^{\frac{2}{3}} \left(\frac{2B(\varepsilon)}{A(\varepsilon) + h^2 C(\varepsilon)} \right)^{\frac{1}{3}} \quad (5.21)$$

and then

$$m_a(\varepsilon, h) = \frac{3}{2^{\frac{2}{3}}} h^{\frac{2}{3}} \left(A(\varepsilon) + h^2 C(\varepsilon) \right)^{\frac{2}{3}} B^{\frac{1}{3}}(\varepsilon). \quad (5.22)$$

Assuming $C(\varepsilon) = O(1)$ as $h \rightarrow 0$, we then have

$$m_a \approx \frac{3}{2^{\frac{2}{3}}} h^{\frac{2}{3}} A^{\frac{2}{3}} B^{\frac{1}{3}} \quad (5.23)$$

and we find by computation of (5.19) that this is minimised when

$$\varepsilon = \varepsilon^* \approx 0.9059. \quad (5.24)$$

Hence $A(\varepsilon^*) = 13.35$, $B(\varepsilon^*) = 4.115 \times 10^{-2}$ and $C(\varepsilon^*) = 8.700$ are $O(1)$. We also note that

$$R^* \rightarrow \left(\frac{2B(\varepsilon^*)}{A(\varepsilon^*)} \right)^{\frac{1}{6}} h^{\frac{1}{3}} \approx 0.4282 h^{\frac{1}{3}}, \quad m_a(h) \approx 3.6718 h^{\frac{2}{3}} \quad (5.25)$$

as $h \rightarrow 0$.

5.3. THE LOWER BOUND

As in the previous section, we imagine the flux tube is bounded by a fluid domain in the form of a sphere. The optimal choice of the radius R' of the sphere is

$$R' = \sqrt{L^2 + R^2(1 + \varepsilon)^2} \approx L \quad (5.26)$$

and therefore, from (4.29),

$$m_a(h) \geq \frac{\pi V^{\frac{1}{3}} |h|}{\sqrt{L^2 + R^2(1 + \varepsilon)^2}} = \frac{\pi |h|}{\sqrt{(8\pi\varepsilon R^2)^{-2} + R^2(1 + \varepsilon)^2}}. \quad (5.27)$$

In the limit $h \rightarrow 0$, $\varepsilon \rightarrow \varepsilon^*$ and $R \rightarrow R^* h^{2/3}$ where ε^* and R^* are constants; hence we have, approximately, that

$$m_a(h) \geq \frac{\pi h^{\frac{5}{3}}}{\sqrt{0.0574 + 0.6660 h^2}} \quad (5.28)$$

for small h . Combining with (5.25), we obtain

$$13.11 h^{\frac{5}{3}} \leq m_a(h) \leq 3.6718 h^{\frac{2}{3}} \quad (5.29)$$

as $h \rightarrow 0$.

6. THE CASE OF $h=O(1)$

In this case numerical methods must be used. The numerical solution of the variational problem (3.19)- (3.20) can be obtained by discretizing the variable $F(\chi, \phi)$ both in χ and in ϕ . For simplicity, however, we restrict $F(\chi, \phi)$ to take the form

$$F(\chi, \phi) = f(\chi) g(\phi) \quad (6.1)$$

where

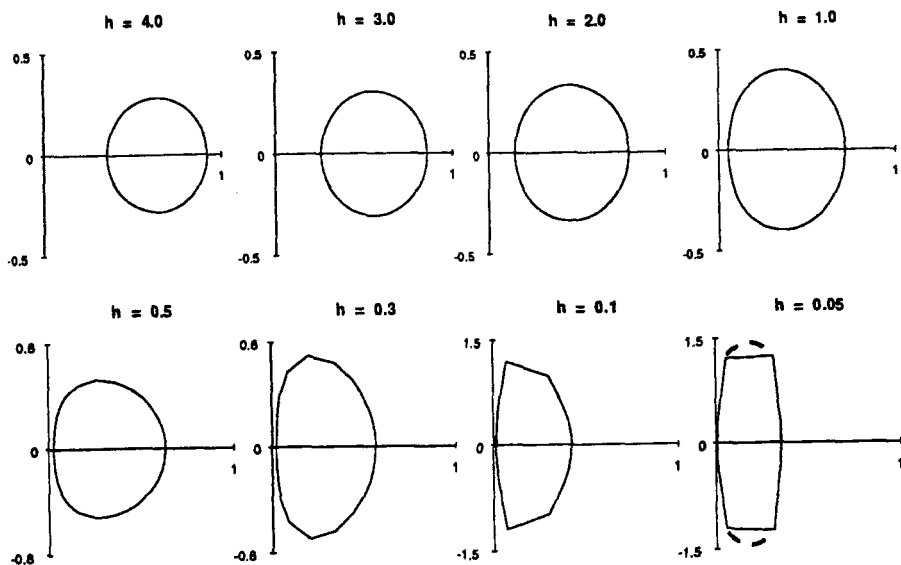


Fig. 5. The cross-section of minimum energy states for various values of h when the boundary is approximated by $(16+1)$ points. Note that the numerical solutions are poor when h is small.

$$f(\chi) = \left(\frac{V\chi}{\pi h \Phi R} \right)^{\frac{1}{2}}. \quad (6.2)$$

The contours of constant χ are then similar in shape; and $f(\chi)$ is chosen to be compatible with the large h results given in section 4. We expect that $g(\phi) \rightarrow 1$ as $h \rightarrow 0$ since in the limit the shape of the cross-section at equilibrium is a circle.

The constraint (3.20) becomes

$$\int_0^{2\pi} (R + fg \cos \phi) g^2 d\phi = 2\pi R \quad (6.3)$$

which is decomposed into

$$\int_0^{2\pi} g^2 d\phi = 2\pi, \quad \int_0^{2\pi} g^3 \cos \phi d\phi = 0. \quad (6.4)$$

The objective function \mathcal{M} can then be expressed in terms of $g(\phi)$ and R , and is minimized subject to the 'realistic conditions'

$$R + f^* g(\phi) \cos \phi > 0, \quad R > 0, \quad g(\phi) > 0 \quad (6.5)$$

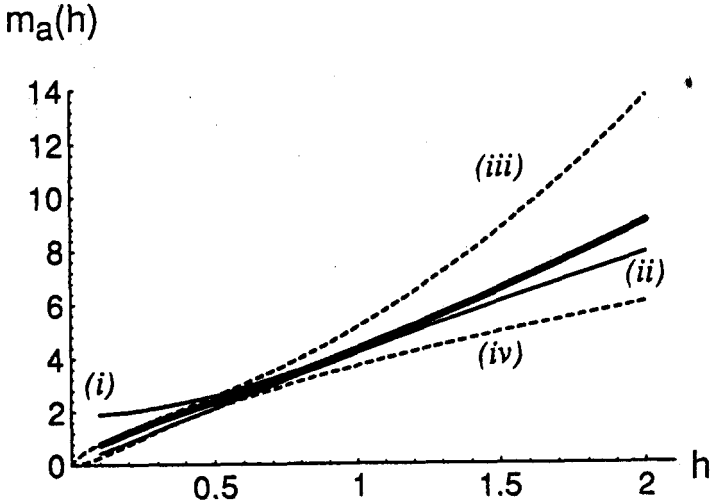


Fig. 6. The minimum energy $m_a(h)$ against h , calculated numerically (thick curve). This plot also shows the estimated (i) upper bound for large h , obtained by numerical minimisation of (4.20); (ii) lower bound for large h , (4.32); (iii) upper bound for small h , obtained by numerical minimisation of (5.22), and (iv) lower bound for small h , (5.28).

where

$$f^* = (2\pi^2 R)^{-\frac{1}{2}} \quad (6.6)$$

(since otherwise the surface is not defined in a meaningful way). The optimization problem is solved by standard numerical routines. Without going into details, we simply state the result in figure 5, which shows the cross-sections for different values of h at relaxed states. Note that the cross-sections deform as h decreases in such a way that magnetic field lines are contracting to the central axis as expected. Also the minimum energy calculated numerically confirms the estimates from previous sections, as summarised in figure 6. Note that $m_a(h)$ has an inflexion point near $h = 1$.

7. THE GRAD-SHAFRANOV EQUATION

Magnetostatic equilibrium with flux function $\chi(r, z)$, pressure field $p = P(\chi)$ and toroidal field $B_\theta(r, z) = r^{-1}F(\chi)$ is governed by the Grad-Shafranov equation

$$D^2\chi = -r^2 P'(\chi) - F(\chi)F'(\chi) \quad (7.1)$$

where

$$D^2 = \frac{\partial^2}{\partial r^2} - \frac{1}{r} \frac{\partial}{\partial r} + \frac{\partial^2}{\partial z^2} . \quad (7.2)$$

When the equilibrium is a circular flux tube of mean radius R and cross-section $A \ll R^2$, the operator D^2 may be approximated by

$$D^2 \approx \frac{\partial^2}{\partial r^2} + \frac{\partial^2}{\partial z^2} \quad (7.3)$$

and the Grad-Shafranov equation may be approximated by

$$\left(\frac{\partial^2}{\partial r^2} + \frac{\partial^2}{\partial z^2} \right) \chi = -R^2 P'(\chi) - F(\chi)F'(\chi) . \quad (7.4)$$

Here, (r, z) may be regarded as cartesian coordinates in the meridian plane, centred on the axis of the flux tube.

Consider now the scale transformation

$$R \rightarrow \lambda R , \quad (r, z) \rightarrow \lambda^{-\frac{1}{2}}(r, z) \quad (7.5)$$

which corresponds to stretching the flux tube by a factor λ and shrinking its cross-section by the same factor to conserve the volume. It may easily be verified that (7.4) is then invariant under the transformation

$$F \rightarrow \lambda^2 F , \quad \chi \rightarrow \lambda^{\frac{3}{2}} \chi \quad \text{and} \quad P \rightarrow \lambda^2 P . \quad (7.6)$$

The toroidal flux Φ_T is invariant under this transformation, but the total poloidal flux, equal to $2\pi\Delta\chi$ where $\Delta\chi$ is the jump in χ from the centre of the flux tube to its boundary, scales as $\Phi_P \sim \lambda^{\frac{3}{2}}$. Hence the helicity scales as

$$\mathcal{H} \sim \Phi_T \Phi_P \sim \lambda^{\frac{3}{2}} \quad (7.7)$$

or equivalently $\lambda \sim \mathcal{H}^{\frac{2}{3}}$. This is the counterpart of the result (4.14), and provides confirmation that the results (4.13)–(4.15) are characteristic of toroidal magnetostatic equilibrium (when $R \gg A^{1/2}$), even when the cross-section of the flux-tube is not circular.

Similarly, in the case of small h , the operator D is approximated by

$$D^2 \approx \frac{\partial^2}{\partial r^2} - \frac{1}{r} \frac{\partial}{\partial r} \quad (7.8)$$

and (7.1) is invariant under the scale transformation

$$r \rightarrow \lambda r , \quad z \rightarrow \lambda^{-2} z ; \quad F \rightarrow \lambda^2 F , \quad \chi \rightarrow \lambda^3 \chi \quad \text{and} \quad P \rightarrow \lambda P . \quad (7.9)$$

This corresponds to stretching the flux tube by a factor λ in the r -direction and compressing it by a factor λ^2 in the z -direction to conserve the volume. The toroidal flux is again invariant under this transformation, but poloidal flux scales as λ^3 . Hence the helicity scales as

$$\mathcal{H} \sim \Phi_T \Phi_P \sim \lambda^3 \quad (7.10)$$

or $\lambda \sim \mathcal{H}^{1/3}$. This is the counterpart of the result (5.25).

8. THE EFFECT OF NON-AXISYMMETRIC INSTABILITY

In this paper we have studied the minimum energy $m_a(h)$ of the twisted flux tube as a function of h . The main result,

$$m_a(h) \sim \begin{cases} 3.67 h^{2/3} & \text{when } h \ll 1, \\ 3.22 h^{4/3} & \text{when } h \gg 1, \end{cases} \quad (8.1)$$

provides a close estimate from above for the minimum energy of the flux tube. We also estimate a lower bound and the results are summarised in figure 6. All calculations assume that the minimum energy state is axisymmetric. However, preliminary calculation suggests that this configuration is, in fact, unstable to kink mode perturbations when h is larger than a critical value of order unity. The flux tube may then relax further to a state with lower energy, and the result (8.1) should therefore be understood as an upper bound of the true minimum energy $m(h)$.

Although we are unable to calculate the exact form of $m(h)$, there is a simple argument suggesting that $m(h) \sim Ch^{4/3}$ when $h \gg 1$, like $m_a(h)$, but with smaller proportionality constant C . Figure 7a shows a generic situation when a twisted flux tube is deformed by kink mode displacement. The total helicity is unchanged, but the twist ingredient is transformed into a torsion ingredient (associated with the torsion of the axis, see Ricca & Moffatt 1992). Figure 7b shows how a flux tube with a large value of h may relax. A possible model for this relaxed state is a twisted cylindrical flux tube, shown in figure 7c, carrying equal and opposite magnetic flux (of magnitude Φ); the corrections at the two ends are negligible when h is large. In cylindrical polar coordinates, let $\mathbf{B} = (0, B_\theta, B_z)$ be the uniform twisted field confined in the cylinder $C = \{(r, \theta, z) : 0 \leq r \leq a, 0 \leq z \leq L\}$ of volume V and area of cross-section $A = \pi a^2$, then

$$|B_z| = 2\Phi/A, \quad B_\theta = 2\pi br\Phi/V \quad (8.2)$$

where b is to be determined. The 'net' axial flux is $\Phi_z = 2\Phi$, and the flux associated with the azimuthal component of the field is

$$|\Phi_\theta| = \frac{\Phi}{V} \iint 2\pi br \, dr \, dz = b\Phi; \quad (8.3)$$

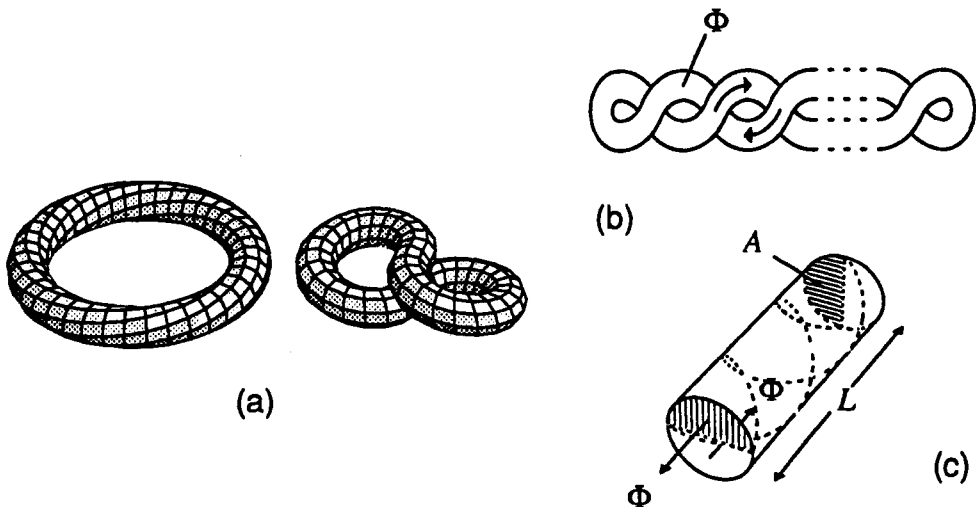


Fig. 7. (a) a torus with twist (of angle 2π) can be deformed into a figure 8 without twist; (b) the non-axisymmetric equilibrium state; (c) the flux tube is approximated by a cylinder with twisted magnetic field.

hence the helicity of the field (8.2) is

$$\mathcal{H} = \Phi_z \Phi_\theta = 2b\Phi^2. \quad (8.4)$$

Since the helicity is an invariant and has the value $h\Phi^2$, therefore $b = h/2$. The magnetic energy is then

$$\mathcal{M} = \frac{1}{2} \int (B_z^2 + B_\theta^2) dV = \Phi^2 \left(\frac{2V}{A^2} + \frac{h^2\pi}{4V} A \right), \quad (8.5)$$

which has a minimum when $A^3 = 16V^2(h^2\pi)^{-1}$, and then, using (4.15),

$$\mathcal{M} = \mathcal{M}_{min} = \frac{3\pi^{\frac{2}{3}}}{2^{\frac{5}{3}}} h^{\frac{4}{3}} \frac{\Phi^2}{V^{\frac{1}{3}}} = \frac{1}{2^{\frac{2}{3}}} m_a(h) \frac{\Phi^2}{V^{\frac{1}{3}}} = m(h) \frac{\Phi^2}{V^{\frac{1}{3}}}, \quad (8.6)$$

where

$$m(h) = 2^{-2/3} m_a(h) \approx 0.63 m_a(h), \quad (8.7)$$

consistent with the conjecture that the relaxed state with lowest energy is non-axisymmetric.

Acknowledgements

A.Y.K.C. would like to thank M.J.D. Powell for his advice on numerical computations; he is also grateful to J. Greene and A. Bhattacharjee for discussions. A.Y.K.C. was supported by the Croucher Foundation.

References

- ARNOL'D, V.I. 1974 The asymptotic Hopf invariant and its applications (in Russian). In *Proc. Summer School in Differential Equations, Erevan*. Armenian SSR Acad. Sci., Transl. 1986 in *Sel. Math. Sov.*, 5, pp. 327-345.
- FREEDMAN, M.H. 1988 A note on topology and magnetic energy in incompressible perfectly conducting fluids. *J. Fluid Mech.*, 194, pp. 549-551.
- KRUSKAL, M.D. & KULSRUD, R.M. 1958 Equilibrium of a magnetically confined plasma in a toroid. *Phys. Fluids*, 1, pp. 265-274.
- MOFFATT, H.K. 1969 The degree of knottedness of tangled vortex lines. *J. Fluid Mech.*, 35, pp. 117-129.
- MOFFATT, H.K. 1985 Magnetostatic equilibria and analogous Euler flows of arbitrary complex topology. Part 1. Fundamentals. *J. Fluid Mech.*, 159, pp. 359-378.
- MOFFATT, H.K. 1990 The energy spectrum of knots and links. *Nature*, 347, pp. 367-369.
- RICCA, R.L. & MOFFATT, H.K. 1992 The helicity of a knotted vortex filament. *This volume*.
- THOMPSON, W.B. 1962 *Introduction to plasma physics*. Pergamon.